We are IntechOpen,
the world's leading publisher of
Open Access books
Built by scientists, for scientists

6,900
Open access books available

185,000
International authors and editors

200M
Downloads

154
Countries delivered to

Our authors are among the

TOP 1%
most cited scientists

12.2%
Contributors from top 500 universities

CLARIVATE ANALYTICS
BOOK CITATION INDEX
INDEXED

WEB OF SCIENCE™

Selection of our books indexed in the Book Citation Index
in Web of Science™ Core Collection (BKCI)

Interested in publishing with us?
Contact book.department@intechopen.com

Numbers displayed above are based on latest data collected.
For more information visit www.intechopen.com

Simulations with Particle Method

Nobuhiko Mukai
Computer Science, Tokyo City University,
Japan

1. Introduction

In computer graphics, one of the most exciting themes is visualization based on physical simulation, and visual simulation of fluid, which includes liquid and air, is the most challenging issue among them. In order to visualize fluid behavior, there are two major methods: Eulerian grid method and Lagrangian particle method. In Eulerian grid method, level set method is used to identify the boundary of the fluid. In Lagrangian particle method, Marching Cubes is used as the technique that generates the surface of the fluid, while some researches use level set method to generate it, which is called particle level set method.

(Greenwood & House, 2004) used particle level set method to visualize bubbles, especially splashing. (Zheng et al., 2006) used a regional level set method with semi-implicit surface tension model to simulate multi-manifold bubbles. (Kim et al., 2007) solved the volume error caused by level set method to visualize foamy bubbles. On the other hand, (Kim et al., 2010) used a spatial averaging and stochastic approach with particles to simulate sparse bubble flow.

In addition, there are two major methods for Lagrangian particle method: SPH (Smoothed Particle Hydrodynamics) and MPS (Moving Particle Semi-implicit) methods. Both methods use particles and calculate fluid behavior based on Navier-Stokes equation; however, the basic idea is different. SPH considers that the physical amount of a particle, which is mass density, velocity and so on, does not belong to the particle itself but it distributes smoothly around the particle, and kernel function is used to calculate the physical amount of each particle. On the other hand, MPS considers that the physical amount such as mass density or velocity belongs to the particle itself, and calculates the interaction between particles with weight function. MPS can also be applied to incompressible fluid by satisfying the condition of density constant.

(Selle et al., 2005) used hybrid techniques of Lagrangian particle method and Eulerian grid based method for vortex visualization. (Hong et al., 2008) also used hybrid method incorporating bubble model based on SPH into Eulerian grid based simulation to visualize bubbly water. In addition, (Chang et al., 2009) used SPH method for viscoelastic fluid simulation. On the other hand, (Yamamoto, 2009) used MPS method to construct momentum preserved two way coupling system between fluids and deformable bodies. The targets of the simulation based on particle method are diverse. The target of most researches mentioned above is bubbles; however, the target of (Chang et al., 2009) is viscoelastic fluids,

and there are many researches on viscoelastic fluids. (Goktekin et al., 2004) used particle level set method to animate incompressible fluids, and visualized the viscoelastic behavior by adding elastic terms to Navier-Stokes equation. On the other hand, (Cavet et al., 2005) used SPH method for fluid simulation, but inserted or removed springs between particles to visualize the behavior of viscoelastic fluid. (Losasso et al., 2006) used separate particle level set method, which sets different levels for multiple regions, to visualize the interaction of different liquids such as viscous objects and water. In addition, (Qin et al., 2010) used a coupling technique of SPH and MSM (Mass Spring Model) to visualize the interaction between blood flow and blood vessel wall

There are many researches using particle method, which are mentioned above; however, the following issues have not been solved. 1) physical based visualization on disappearance of bubbles, 2) visualization of spinnability, which is a character that viscoelastic liquid stretches very thin and long such as a rubber string, and 3) simulation of bleeding out of blood vessel. In addition, SPH is more used than MPS for particle method although MPS can be applied to incompressible fluid. Therefore, in this chapter, MPS based simulation methods for the above unsolved three visualizations are explained.

2. Governing equations

The first basic equation of fluid is equation of continuity that is derived from the law of conservation of mass. Suppose that ρ and m are the density and the mass of fluid, which volume is V. Then, the following equation is true.

$$m = \int_V \rho dV \tag{1}$$

If mass is constant, the following equation is true since mass is invariant for time.

$$\frac{Dm}{Dt} = \frac{D}{Dt} \int_V \rho dV = 0 \tag{2}$$

Where, D/Dt is called Lagrange differential calculus that is defined as follows.

$$\frac{D}{Dt} := \frac{\partial}{\partial t} + \mathbf{u} \cdot \nabla \tag{3}$$

Where, $\mathbf{u}$ is the velocity of fluid and ∇ is gradient. They are defined as follows.

$$\mathbf{u}\left(u_x, u_y, u_z\right) := \left(\frac{\partial x}{\partial t}, \frac{\partial y}{\partial t}, \frac{\partial z}{\partial t}\right) \qquad \nabla := \left(\frac{\partial}{\partial x}, \frac{\partial}{\partial y}, \frac{\partial}{\partial z}\right) \tag{4}$$

Here, Eq. (2) is rewritten as the following by using Reynolds' transport theorem.

$$\int_V \left[\frac{D\rho}{Dt} + \rho \nabla \cdot \mathbf{u}\right] dV = 0 \tag{5}$$

Where, $\nabla \cdot$ is divergence that is defined as follows.

$$\nabla \cdot := \frac{\partial}{\partial x} + \frac{\partial}{\partial y} + \frac{\partial}{\partial z} \tag{6}$$

Eq. (5) should be approved for any volume so that equation of continuity is derived as the following (Nakamura, 1997).

$$\frac{D\rho}{Dt} + \rho\nabla \cdot \mathbf{u} = 0 \quad or \quad \frac{\partial\rho}{\partial t} + \nabla \cdot (\rho\mathbf{u}) = 0 \tag{7}$$

If fluid is incompressible, ρ is also invariant for time so that equation of continuity for incompressible fluid becomes Eq. (8).

$$\nabla \cdot \mathbf{u} = 0 \tag{8}$$

The next important equation is Cauchy's equation of motion that is derived from the law of conservation of momentum, which is defined as follows (Nakamura, 1997).

$$\frac{D}{Dt}\int_V \rho\mathbf{u}dV = \int_S \mathbf{n} \cdot \boldsymbol{\sigma}dS + \int_V \rho\mathbf{K}dV \tag{9}$$

Where, $\mathbf{n}$ is normal vector of the surface, $\boldsymbol{\sigma}$ is stress tensor, and $\mathbf{K}$ is body force per unit mass. Eq. (9) can be rewritten as follows by using Reynolds' transport theorem and Gauss' divergence theorem.

$$\int_V \left[\frac{D(\rho\mathbf{u})}{Dt} + \rho\mathbf{u}\nabla \cdot \mathbf{u} \right] dV = \int_V \nabla \cdot \boldsymbol{\sigma}dS + \int_V \rho\mathbf{K}dV \tag{10}$$

Then, Cauchy's equation of motion is derived as follows from Eq. (10) by considering equation of continuity (Eq. (7)).

$$\rho\frac{D\mathbf{u}}{Dt} = \nabla \cdot \boldsymbol{\sigma} + \rho\mathbf{K} \tag{11}$$

The last important equation of fluid is Navier-Stokes equation, which is derived from Cauchy's equation of motion. Here, stress tensor is described as follows by using pressure p, unit tensor $\mathbf{I}$ and stress deviation $\boldsymbol{\tau}$ (Nakamura, 1997).

$$\boldsymbol{\sigma} = -p\mathbf{I} + \boldsymbol{\tau} \tag{12}$$

In addition, stress deviation can be rewritten as follows for incompressible fluid.

$$\boldsymbol{\tau} = 2\mu\mathbf{D} \tag{13}$$

Where, μ is coefficient of viscosity, $\mathbf{D}$ is deformation rate tensor and written as follows with element expression.

$$D_{ii} := \frac{\partial u_i}{\partial x_i} := \frac{\partial u_1}{\partial x_1} + \frac{\partial u_2}{\partial x_2} + \frac{\partial u_3}{\partial x_3}, \qquad D_{ij} = D_{ji} = \frac{1}{2}\left(\frac{\partial u_i}{\partial x_j} + \frac{\partial u_j}{\partial x_i} \right) \tag{14}$$

Where, the suffix of i and j represents 1, 2 or 3, in turn, 1, 2 and 3 represents x, y and z, respectively. With the above equations (Eq. (8), (11), (12), (13) and (14)), Navier-Stokes equation is derived as the following (Nakamura, 1997)..

$$\rho\frac{D\mathbf{u}}{Dt} = -\nabla p + \mu\nabla^2\mathbf{u} + \rho\mathbf{K} \tag{15}$$

Where, ∇^2 is Laplacian and defined as follows.

$$\nabla^2 := \frac{\partial^2}{\partial x_i^2} := \frac{\partial^2}{\partial x_1^2} + \frac{\partial^2}{\partial x_2^2} + \frac{\partial^2}{\partial x_3^2} = \frac{\partial^2}{\partial x^2} + \frac{\partial^2}{\partial y^2} + \frac{\partial^2}{\partial z^2} \tag{16}$$

3. MPS method

As mentioned above, there are two major particle methods: SPH and MPS. SPH considers that the physical amount of a particle distributes smoothly around the particle, while MPS considers that the physical amount of a particle belongs to the particle itself, and calculates the interaction between particles with weight function. If the calculation is performed for all particles, it takes huge amount of time so that MPS limits the area for the calculation of one particle, and considers that only particles within the area affect the interaction for the particle. The radius of the area, which is defined as a sphere, is called the radius of influence. Fig. 1 illustrates the radius of influence for particle i as r_e and one of particles affecting particle i as j. The quantity affecting from particle j to particle i is calculated with weight function shown in Eq. (17).
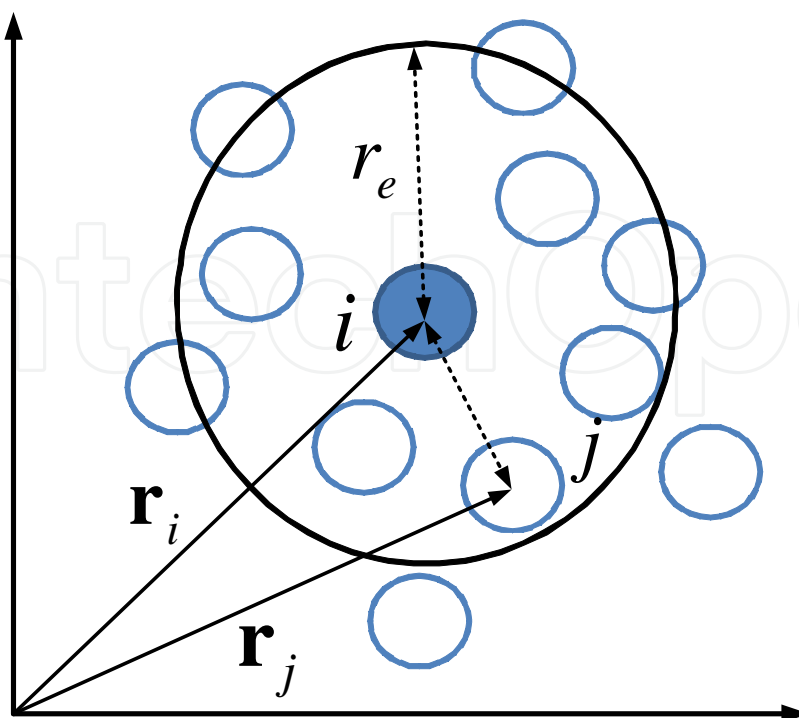

Fig. 1. Relation between a particle and the radius of influence

$$w\left(\left|\mathbf{r}_j - \mathbf{r}_i\right|\right) = \begin{cases} \dfrac{r_e}{|\mathbf{r}_j - \mathbf{r}_i|} - 1 & \left(0 < |\mathbf{r}_j - \mathbf{r}_i| < r_e\right) \\ \\ 0 & \left(r_e \leq |\mathbf{r}_j - \mathbf{r}_i|\right) \end{cases} \tag{17}$$

Where, $|\mathbf{r}_j - \mathbf{r}_i|$ is the distance between particle i and particle j. In addition, the density n_i in the area, which is a sphere that has particle i as the center and the radius of influence r_e as its radius, is called particle number of density and calculated with the above weight function as follows.

$$n_i = \sum_{j \neq i} w\left(\left|\mathbf{r}_j - \mathbf{r}_i\right|\right) \tag{18}$$

Especially, the initial density is expressed as n^0, and this value is kept constantly for incompressible fluid during simulation. In MPS method, discrete operators for gradient, divergence and Laplacian are defined as follows in order to solve Navier-Stokes equation.

$$\text{Gradient: } \langle \nabla \phi \rangle_i = \frac{d}{n^0} \sum_{j \neq i} \left[\frac{\phi_j - \phi_i}{\left|\mathbf{r}_j - \mathbf{r}_i\right|^2} \left(\mathbf{r}_j - \mathbf{r}_i\right) w\left(\left|\mathbf{r}_j - \mathbf{r}_i\right|\right) \right] \tag{19}$$

$$\text{Divergence: } \langle \nabla \cdot \mathbf{u} \rangle_i = \frac{d}{n^0} \sum_{j \neq i} \frac{\left(\mathbf{u}_j - \mathbf{u}_i\right) \cdot \left(\mathbf{r}_j - \mathbf{r}_i\right)}{\left|\mathbf{r}_j - \mathbf{r}_i\right|^2} w\left(\left|\mathbf{r}_j - \mathbf{r}_i\right|\right) \tag{20}$$

$$\text{Laplacian: } \langle \nabla^2 \phi \rangle_i = \frac{2d}{\lambda n^0} \sum_{j \neq i} \left[\left(\phi_j - \phi_i\right) w\left(\left|\mathbf{r}_j - \mathbf{r}_i\right|\right) \right] \tag{21}$$

$$\lambda = \frac{\displaystyle\sum_{j \neq i} \left|\mathbf{r}_j - \mathbf{r}_i\right|^2 w\left(\left|\mathbf{r}_j - \mathbf{r}_i\right|\right)}{\displaystyle\sum_{j \neq i} w\left(\left|\mathbf{r}_j - \mathbf{r}_i\right|\right)} \tag{22}$$

Where, ϕ_i and $\mathbf{u}_i$ are quantities of scalar such as density, and vector such as velocity for particle i respectively, and d is the space dimension number (Koshizuka, 2005).

MPS method treats incompressible fluid so that the density should be preserved, which means that particle number n_i should be kept to be the same as the initial particle number n^0. In order to perform it, all terms except for the pressure are calculated at first, and then, particles move to temporal positions according to the velocities that are also calculated temporarily. Next, the pressure term is calculated by solving Poisson equation of pressure. Then, particle velocities and positions are modified by calculating the velocity again with the pressure term. Finally, fluid is visualized by generating polygons from particles with some methods such as Marching Cubes or particle level set method.

Here, how to derive Poisson equation of pressure is explained. At first, all terms except for pressure are considered for Navier-Stokes equation so that only pressure term should be

considered this time. Navier-Stokes equation with only the pressure term is written as Eq. (23).

$$\rho\frac{D\mathbf{u}}{Dt} = -\nabla p \tag{23}$$

In addition, MPS supposes incompressible fluid so that the density is constant. Then, the equation of continuity (Eq. (7)) is written as follows with the initial density of ρ^0.

$$\frac{D\rho}{Dt} + \rho^0\nabla\cdot\mathbf{u} = 0 \tag{24}$$

In MPS, the density is calculated as particle number with Eq. (18). Then, Eq. (24) can be written as Eq. (25).

$$\frac{1}{n^0}\frac{n^0 - n^*}{\Delta t} + \nabla\cdot\mathbf{u} = 0 \tag{25}$$

Here, n^* is the temporal density. Eq. (23) can also be written as follows since Eq. (8) is satisfied for incompressible fluid.

$$-\nabla p = \rho\left(\frac{\partial\mathbf{u}}{\partial t} + \mathbf{u}\nabla\cdot\mathbf{u}\right) = \rho^0\frac{\partial\mathbf{u}}{\partial t} \tag{26}$$

Then, the velocity can be expressed as follows.

$$\mathbf{u} = -\frac{\Delta t}{\rho^0}\nabla p \tag{27}$$

Finally, by substituting Eq. (27) for Eq. (25), Poisson equation of pressure is obtained as the following (Koshizuka, 2005).

$$\nabla^2 p = -\frac{\rho^0}{\Delta t^2}\frac{n^* - n^0}{n^0} \tag{28}$$

The simulation algorithm by MPS method is shown in Fig. 2.

4. Bubble simulation

This simulation supposes that fluid velocity is low and bubbles appear at a depth of about a few centimeters. Then, fluid is supposed to be incompressible so that MPS method is applied. In addition, the analysis method of two dimensional simulation is described for easy understanding. Fig. 3 shows the bubble model. There are many water particles in the water and some air particles make a bubble. The bubble in the water moves up to water surface by the pressure difference among particles. In Fig. 3, the pressure of a particle that constructs the lower part of the bubble, which is shown as P_B in Fig. 3, is higher than the pressure of a particle that constructs the upper part of the bubble, which is shown as P_A in Fig. 3, so that the bubble moves up to water surface. After it reaches water surface, a
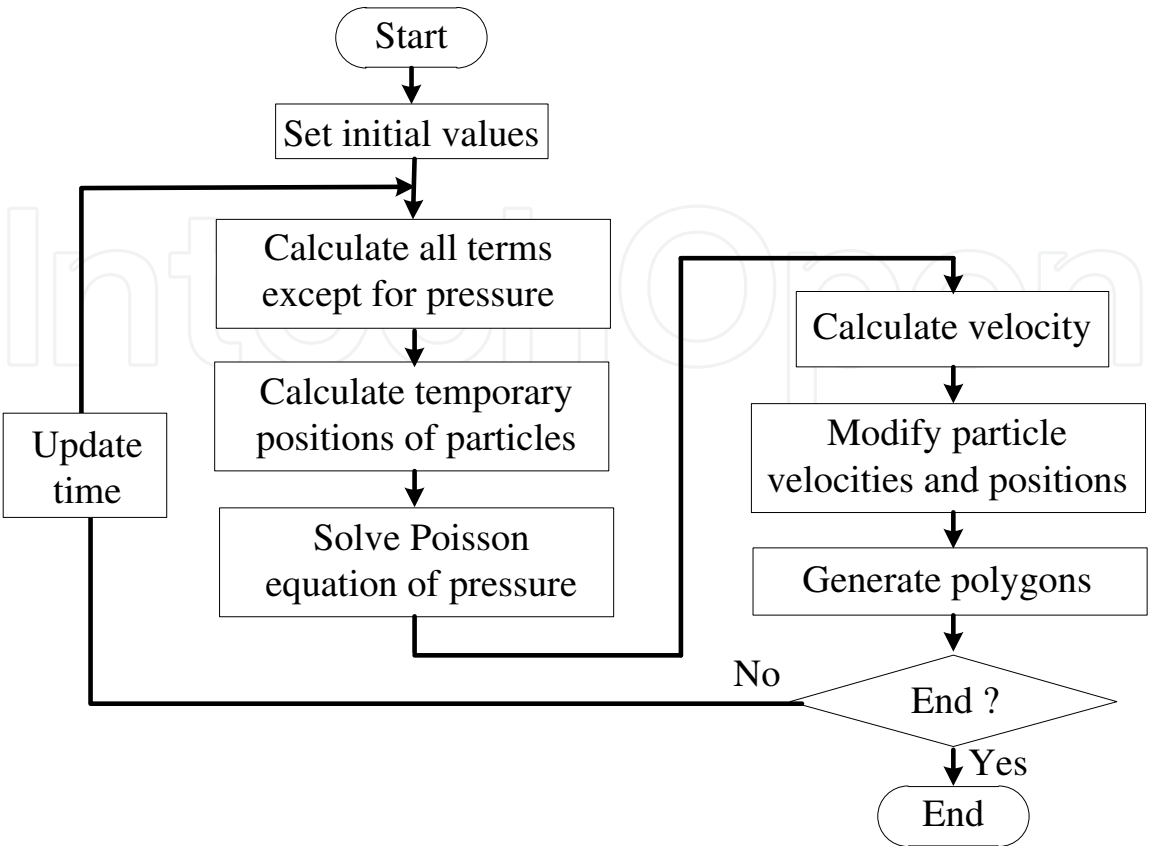
Fig. 2. Simulation algorithm using MPS

part of the bubble goes out of the water and this part is called water screen that is constructed with water screen particles. The bubble that has went out of the water still moves up by surface tension that works on water screen particle. Finally, the pressure difference between the inside and the outside of the bubble becomes larger than the surface tension. Then, the bubble is broken and dissappears. This is the bubble model of this simulation. Therefore, the governing equations of bubble simulation are equation of continuity (Eq. (7)) and Navier-Stokes equation with surface tension shown as the following.

$$\rho \frac{D\mathbf{u}}{Dt} = -\nabla p + \mu \nabla^2 \mathbf{u} + \rho \mathbf{K} + \gamma \kappa \delta \mathbf{n} \tag{29}$$

Where, γ is surface tension coefficient, κ is curvature, δ is delta function, $\mathbf{n}$ is normal vector of surface tension on water screen.

Water screen particle is different from a particle that is inside water particles, and is called free surface particle. It means that water screen particle is one of free surface particles. Then, free surface particle should be searched in order to find water screen particle. Free surface particle is not inside water particles but on the surface of water particles, so that particle number of density is low. In this simulation, fluid is supposed to be incompressible so that particle number of density is constant and the same as the initial one. Then, a particle, which particle number of density is less than 97% of the initial density, is defined as free surface particle.
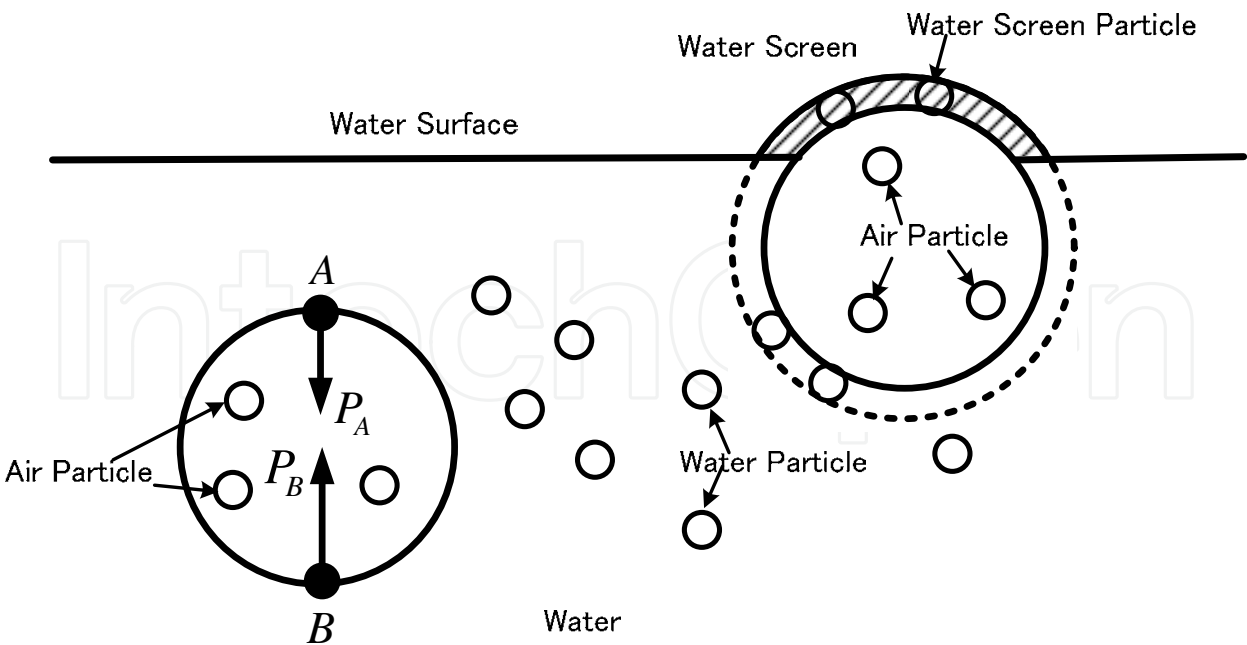
Fig. 3. Bubble model

Next, the calculation of surface tension is described. Surface tension is caused by bonding strength between water particles. Then, it is necessary to calculate the density of water screen, and the density in MPS is considered as the particle number so that particles that are within the radius of influence of a particle, should be counted to calculate the density. The particle density is calculated as follows.

$$w^{st}\left(\left|\mathbf{r}_j - \mathbf{r}_i\right|\right) = \begin{cases} 1 & \left(0 < |\mathbf{r}_j - \mathbf{r}_i| < r_e\right) \\ 0 & \left(r_e \leq |\mathbf{r}_j - \mathbf{r}_i|\right) \end{cases} \tag{30}$$

$$+ n_i^{st} = \sum_{j \neq i} w^{st}\left(\left|\mathbf{r}_j - \mathbf{r}_i\right|\right) \tag{31}$$

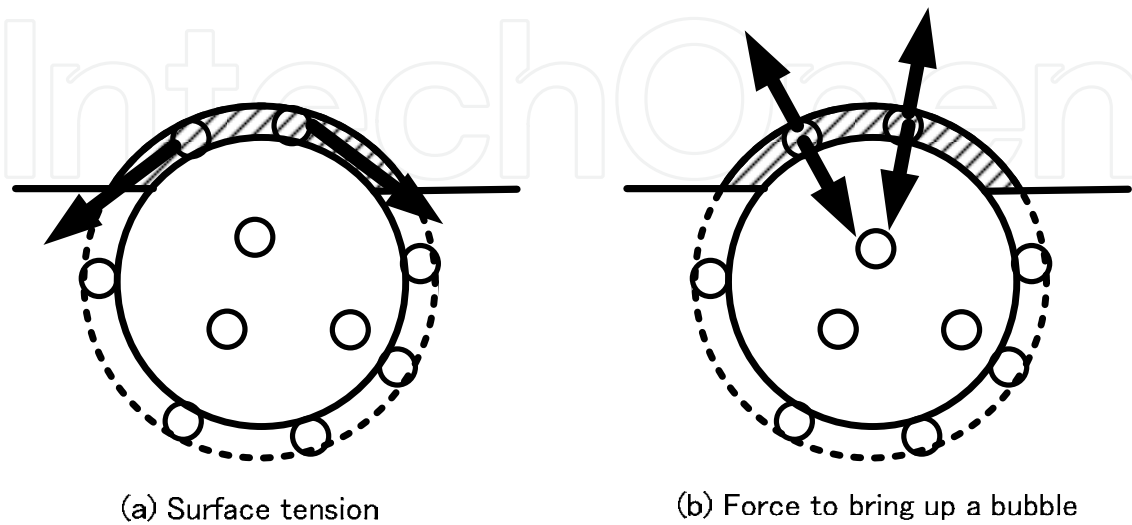(a) Surface tension   (b) Force to bring up a bubble

Fig. 4. Surface tension and force to bring up a bubble

Then, normal vector **n** of surface tension for a particle is calculated by the difference of the densities around the particle. The direction of surface tension, which is calculated with the above method, is shown in Fig. 4 (a). The surface tension is on water screen and facing out of the bubble. Bubbles move up out of the water and dissappear eventually; however, this force cannot bring up the bubble. Then, our method counts not only water particles but also air particles that are in the bubble for the calculation of particle density. By counting the air particles, the direction of surface tension faces the inside of water screen, and the reaction of this surface tension brings up the bubble (Fig. 4 (b)).

Fig. 5 shows a result of the simulation, where a bubble moves up to water surface from the bottom of the water. The model is constructed with 1,232 particles, where 756, 60, and 416 particles for water, air and wall, respectively. On the way to water surface, the shape of the bubble changes by the pressure from the water particles around the bubble. After the bubble

(a) after 0.03 second   (b) after 0.06 second   (c) after 0.09 second

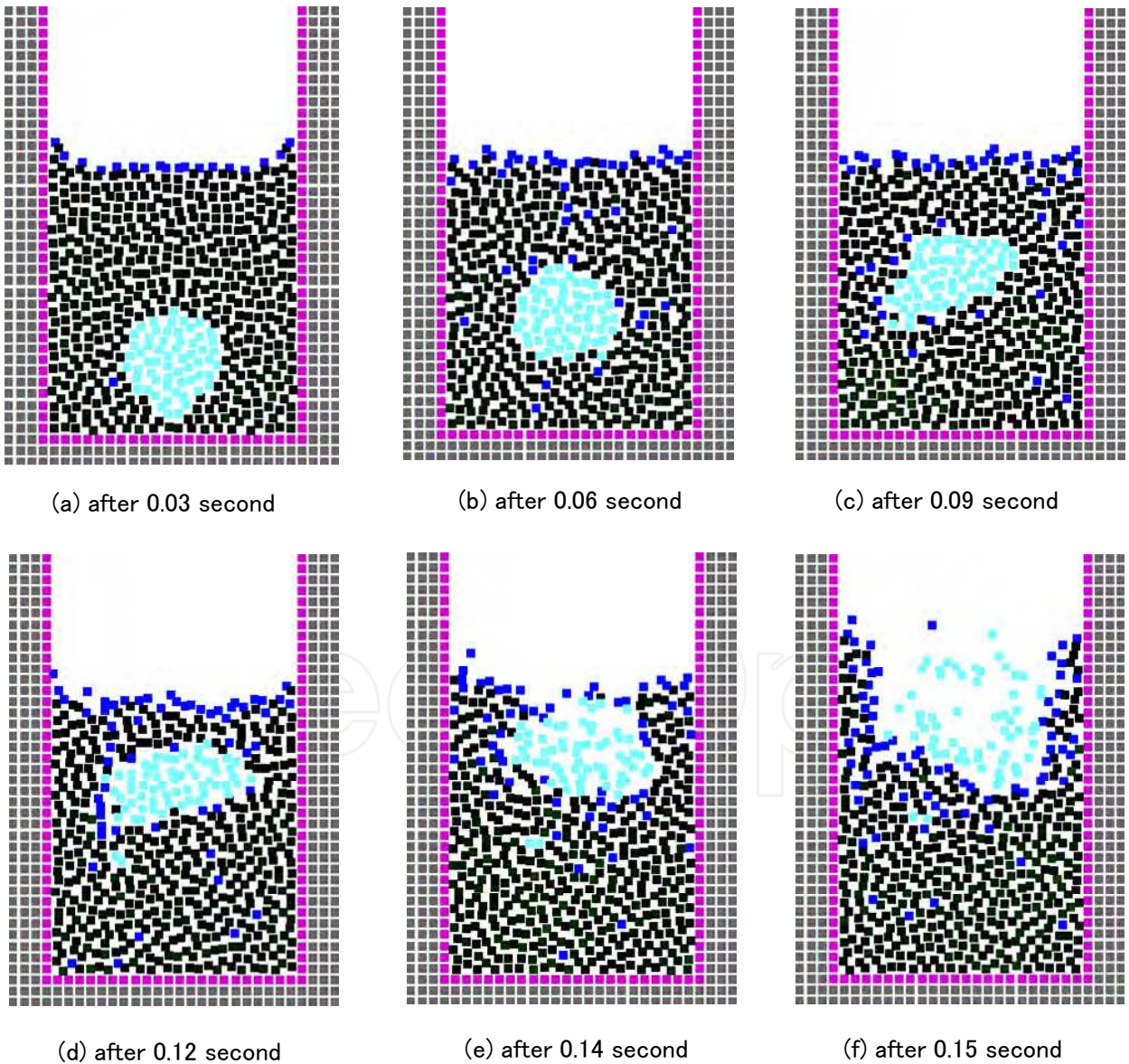(d) after 0.12 second   (e) after 0.14 second   (f) after 0.15 second

Fig. 5. A bubble moving up from the bottom of the water (with surface tension).

reaches water surface, the reaction of the surface tension brings up the bubble, and water screen is broken when the pressure inside the bubble is higher than the surface tension of water screen. Finally, the bubble disappears.

On the other hand, Fig. 6 shows another result of the simulation without surface tension. If there is no surface tension, the bubble cannot keep its shape, and air particles inside the bubble diffuse in the water. The bubble is broken before it reaches water surface (Kagatsume et al., 2011).
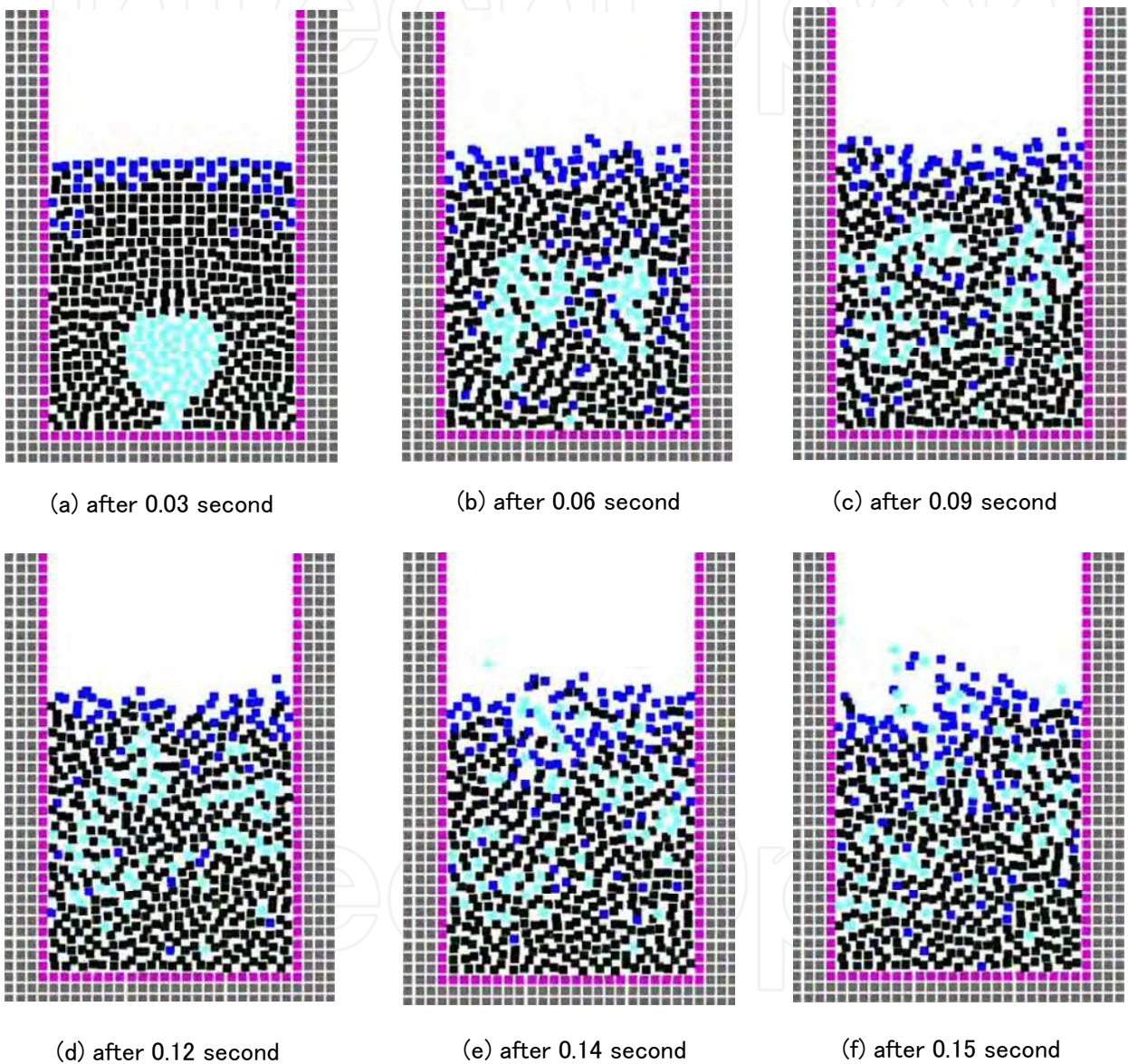

(a) after 0.03 second   (b) after 0.06 second   (c) after 0.09 second

(d) after 0.12 second   (e) after 0.14 second   (f) after 0.15 second

Fig. 6. A bubble moving up from the bottom of the water (without surface tension).

5. Spinnability simulation

Spinnability is one feature of viscoelastic fluid, which has a character of both viscosity and elasticity. When viscoelastic fluid is pulled, it stretches very thin and long such as a rubber string. This feature is called spinnability. For spinnability simulation, equation of continuity is

necessary and also Navier-Stokes equation is used; however, constitutive equation of viscoelastic fluid should be taken into account for stress tensor of Cauchy's equation of motion. Then, in this section, governing equations are derived from Cauchy's equation of motion. In addition, when viscoelastic fluid is stretched, it has free surface so that surface tension should be considered. Then, Cauchy's equation of motion with surface tension is the following.

$$\rho \frac{D\mathbf{u}}{Dt} = \nabla \cdot \boldsymbol{\sigma} + \rho \mathbf{K} + \gamma \kappa \delta \mathbf{n} \tag{32}$$

Here, stress tensor can be written as $\boldsymbol{\sigma} = -p\mathbf{I} + \boldsymbol{\tau}$ (Eq. (12)). For viscoelastic fluid, stress deviation $\boldsymbol{\tau}$ is divided into two parts: viscoelastic fluid and solvent as follows because viscoelastic fluid is dissolved by solvent in order to have the feature of spinnability.

$$\boldsymbol{\tau} = \boldsymbol{\tau}_v + \boldsymbol{\tau}_s \tag{33}$$

Solvent is incompressible fluid so that the stress deviation is written as follows by Eq. (13).

$$\boldsymbol{\tau}_s = 2\mu_s \mathbf{D} \tag{34}$$

On the other hand, there are some models for stress deviation of viscoelastic fluid, and two models, which are Giesekus and Larson models, are adopted and compared in this section.

Giesekus model:

$$\boldsymbol{\tau}_v + \lambda \stackrel{\triangledown}{\boldsymbol{\tau}_v} + \alpha \frac{\lambda}{\mu_v} \boldsymbol{\tau}_v \cdot \boldsymbol{\tau}_v = 2\mu_v \mathbf{D} \tag{35}$$

Larson model:

$$\boldsymbol{\tau}_v + \lambda \stackrel{\triangledown}{\boldsymbol{\tau}_v} + \frac{2\zeta\lambda}{3G} \mathbf{D} : \boldsymbol{\tau}_v (\boldsymbol{\tau}_v + G) = 2\mu_0 \mathbf{D} \tag{36}$$

Where, λ is relaxation time, α is influence coefficient of nonlinear term, ζ is model parameter, G is relaxation modulus, μ_0 is zero shear viscosity, : is inner product of tensor. In addition, $\triangledown$ in the above equations (Eq. (32) and (33)) is called upper convective difference and defined as follows.

$$\stackrel{\triangledown}{\boldsymbol{\tau}_v} = \frac{d\boldsymbol{\tau}_v}{dt} - \mathbf{L} \cdot \boldsymbol{\tau}_v - \boldsymbol{\tau}_v \cdot \mathbf{L}^t \tag{37}$$

$$\mathbf{D} = \frac{1}{2}\left(\mathbf{L} + \mathbf{L}^t\right), \quad \mathbf{L} = \nabla \mathbf{u} \tag{38}$$

Fig. 7 shows particle model expression of spinability simulation with Giesekus model. Fig. 7 (a) shows the initial state. The model is composed of 2,744 particles for viscoelastic fluid and 5,007 particles for solid objects, which are just attached with the viscoelastic fluid and pulled. Then, the viscoelastic fluid is stretched according to the movement of solid objects. Fig. 7 (b) shows the middle state, where the viscoelastic fluid is stretching such as a rubber string. The middle part of the fluid is gradually thinner. Fig. 7 (c) shows the state just before

it is broken so that there are only a few particles at the thinnest part. Fig. 7 (d) shows the state just after it is broken, then the fluid shrinks rapidly as if it is a rubber string. In turn, Fig. 8 shows the surface model expression of the same particle model from the different point of view. Surface model is generated from the particle model with Marching Cubes (Mukai et al., 2010).
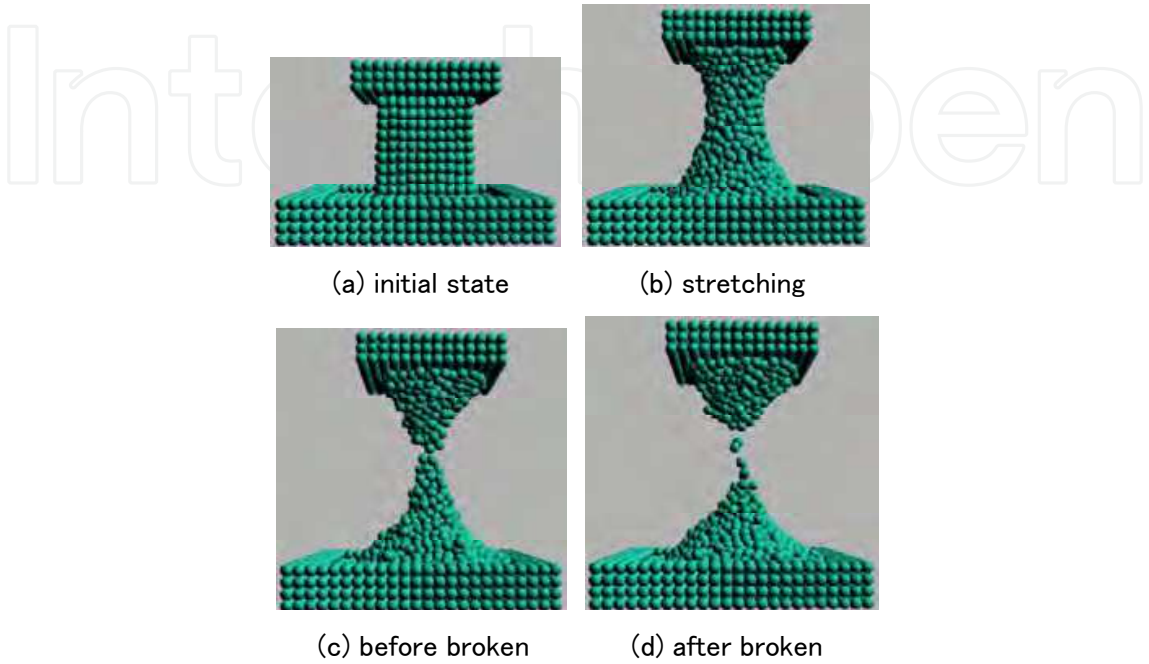

(a) initial state   (b) stretching

(c) before broken   (d) after broken

Fig. 7. Particle model expression of spinability simulation with Giesekus model

(a) initial state   (b) stretching

(c) before broken   (d) after broken

Fig. 8. Surface model expression of spinability simulation with Giesekus model

(a) initial state   (b) stretching

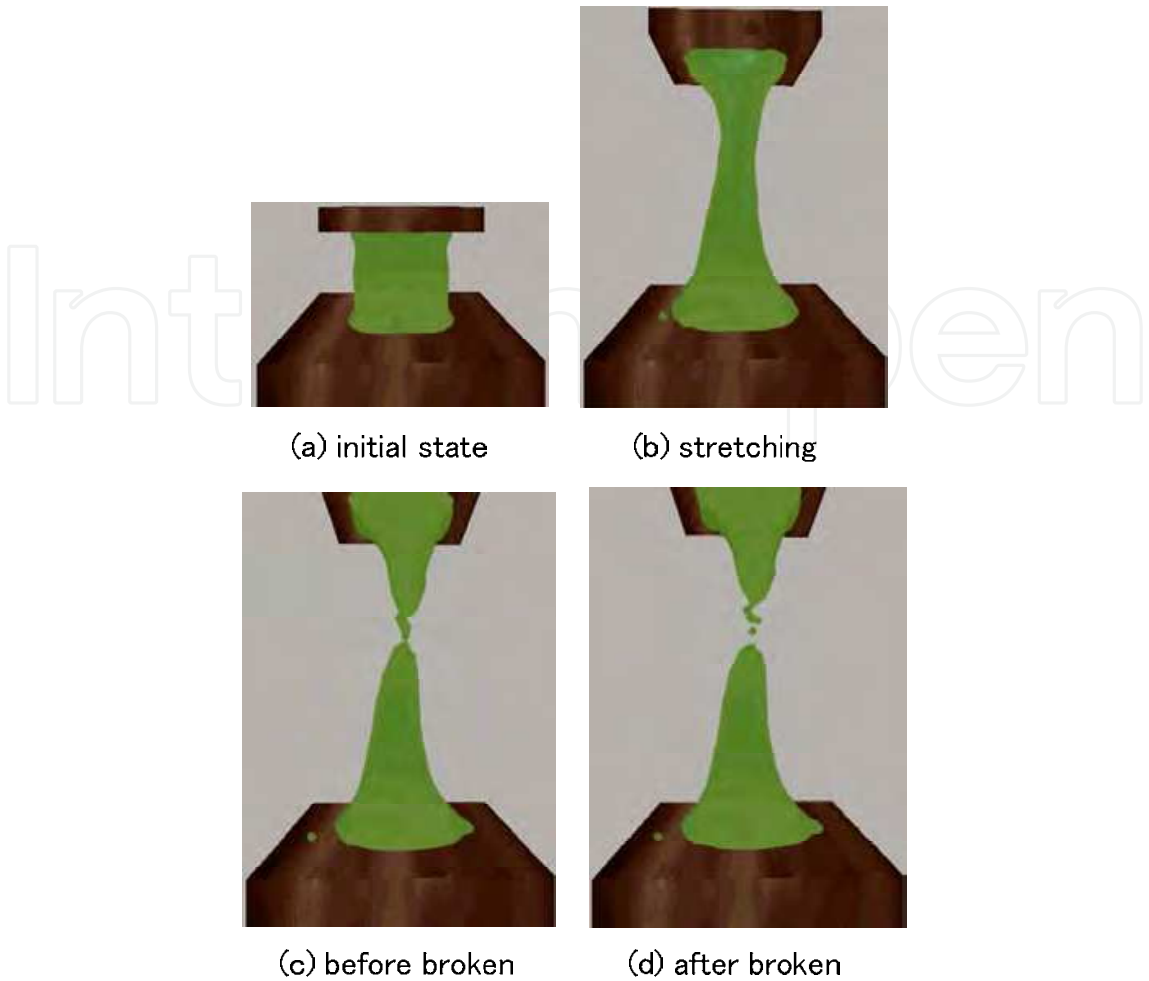(c) before broken   (d) after broken
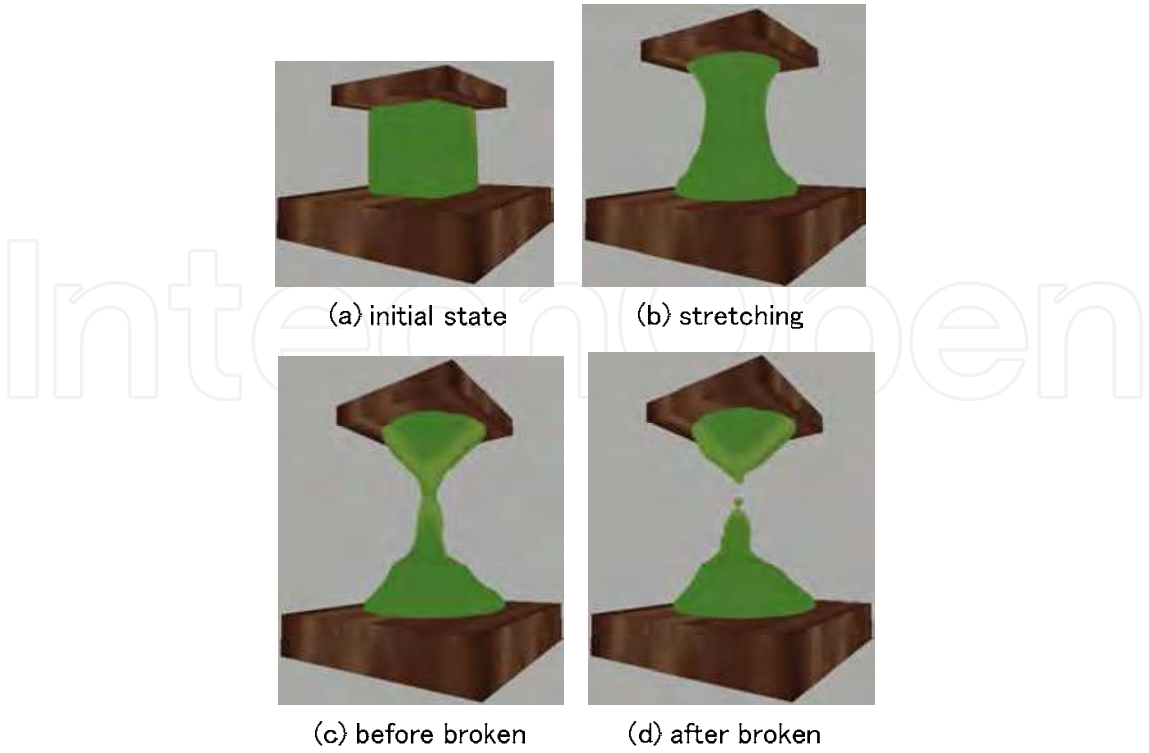
Fig. 9. Surface model expression of spinability simulation with Larson model

On the other hand, Fig. 9 shows surface model expression with Larson model. The viscoelastic fluid with Larson model is more stretching than that with Giesekus model. The stretching length depends on the velocity of viscoelastic fluid. Table 1 shows the comparison of the stretching length for Giesekus and Larson models according to its velocity. The viscoelastic fluid with Giesekus model does not stretch so much for the velocity, while the fluid with Larson model stretches longer for the velocity (Arimatsu et al., 2011).

Velocity [m/s]	Stretching length [mm]	
	Giesekus model	Larson model
0.018	2.3	14.7
0.068	2.3	21.4
0.100	2.4	22.8
0.140	2.4	25.8
0.180	2.4	28.4

Table 1. Comparison of the stretch length

6. Blood flow simulation

This section explains the method of blood vessel deformation and bleeding simulation by using MPS. Blood itself is fluid so that it should be simulated with particle model. On the other hand, blood vessel is not fluid but solid that deforms very easily, which is elastic body. In addition, we have to consider the interaction between blood flow and blood vessel. Then, in this section, blood vessel is decomposed into small particles and the interaction between blood itself and blood vessel is calculated with particle method. The governing equations are equation of continuity (Eq. (7)) and Cauchy's equation of motion (Eq. (11)). For incompressible fluid, the stress tensor $\boldsymbol{\sigma}$ is expressed as follows with Eq. (12) and (13).

$$\boldsymbol{\sigma} = -p\mathbf{I} + 2\mu\mathbf{D} \tag{39}$$

On the other hand, the stress tensor $\boldsymbol{\sigma}$ for elastic body is expressed as follows.

$$\boldsymbol{\sigma} = -\lambda tr(\boldsymbol{\varepsilon})\mathbf{I} + 2G\boldsymbol{\varepsilon} \tag{40}$$

Where, $\boldsymbol{\varepsilon}$ is strain tensor, λ and G are Lame parameters that are defined as follows.

$$\lambda = \frac{\nu E}{(1+\nu)(1-2\nu)}, \quad G = \frac{E}{2(1+\nu)} \tag{41}$$

Where, ν is Poisson's ratio and E is Young's modulus. Trace of strain tensor $tr(\boldsymbol{\varepsilon})$ is calculated as the difference between particle number of density and initial one as follows.

$$\langle tr(\boldsymbol{\varepsilon}) \rangle_i = -\frac{n_i - n^0}{n_i} \tag{42}$$

In addition, non-slip boundary condition is satisfied for the boundary between the blood vessel and blood particles that touch the blood vessel. The interaction force $\mathbf{F}$ between particles is calculated with Hooke's law as follows.

$$F_{\mathbf{i}} = \begin{cases} \sum_{i \neq j} k \dfrac{\left(\left|\mathbf{r}_j - \mathbf{r}_i\right|\right)}{2r} & \left(\left|\mathbf{r}_j - \mathbf{r}_i\right| < 2r\right) \\ 0 & \left(r \leq \left|\mathbf{r}_j - \mathbf{r}_i\right|\right) \end{cases} \tag{43}$$

Where, k is spring constant and r is the radius of a particle.

Fig. 10 shows the simulation result of blood vessel deformation. Fig. 10 (a) shows the initial state, where two surgical tools are supporting a blood vessel model lying horizontally. The number of particles for the blood vessel, blood and surgical tools are 9,568, 5,852 and 1,365, respectively. Fig. 10 (b) shows the case that the inside of the blood vessel is filled with elastic particles so that the blood vessel is not deformed so much when two surgical tools push the blood vessel. On the contrary, Fig. 10 (c) shows the case that the inside of the blood vessel is empty so that the blood vessel is deformed largely; however, it is not real because there is blood flow inside the blood vessel. Then, Fig. 10 (d) shows the case that the inside of the

blood vessel is filled with blood particles so that the blood vessel is deformed moderately, since there is blood flow inside the blood vessel and the blood flow pressure pushes back the force that comes from the surgical tools.
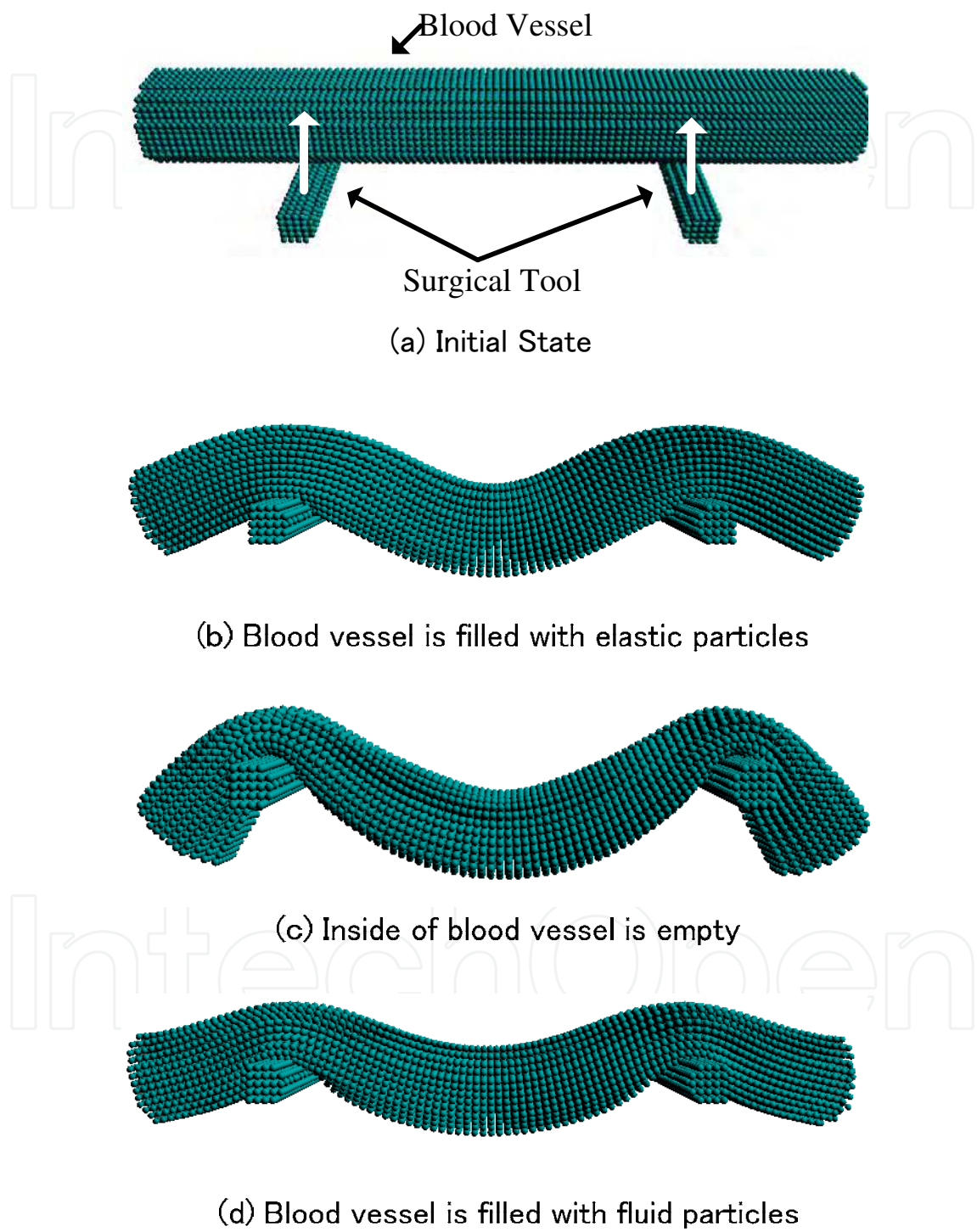

(a) Initial State

(b) Blood vessel is filled with elastic particles

(c) Inside of blood vessel is empty

(d) Blood vessel is filled with fluid particles

Fig. 10. Blood vessel deformation with particle method

On the other hand, Fig. 11 shows another simulation of blood vessel deformation and bleeding with the aorta model. Fig. 11 (a) shows the initial state. The model is constructed with 15,000

and 7,000 particles for blood vessel and blood itself, respectively. The aorta model is generated from image data of a real patient. The aorta is extracted from volume data, which is constructed with multiple image data, and it is converted into polygon data by using Marching Cubes. Then, the polygon data is converted into particle data, which is used for this simulation. Blood flows into the blood vessel from the upper part of the aorta, and it flows out of the lower part of it. When two surgical tools push the blood vessel, it is deformed by considering the interaction between blood vessel and blood flow (Fig. 11 (b)). In addition, if a part of the blood vessel is broken, bleeding occurs (Fig. 11 (c)). (Nakagawa et al., 2010, 2011)

    (a) Initial State   (b) Deformation   (c) Bleeding
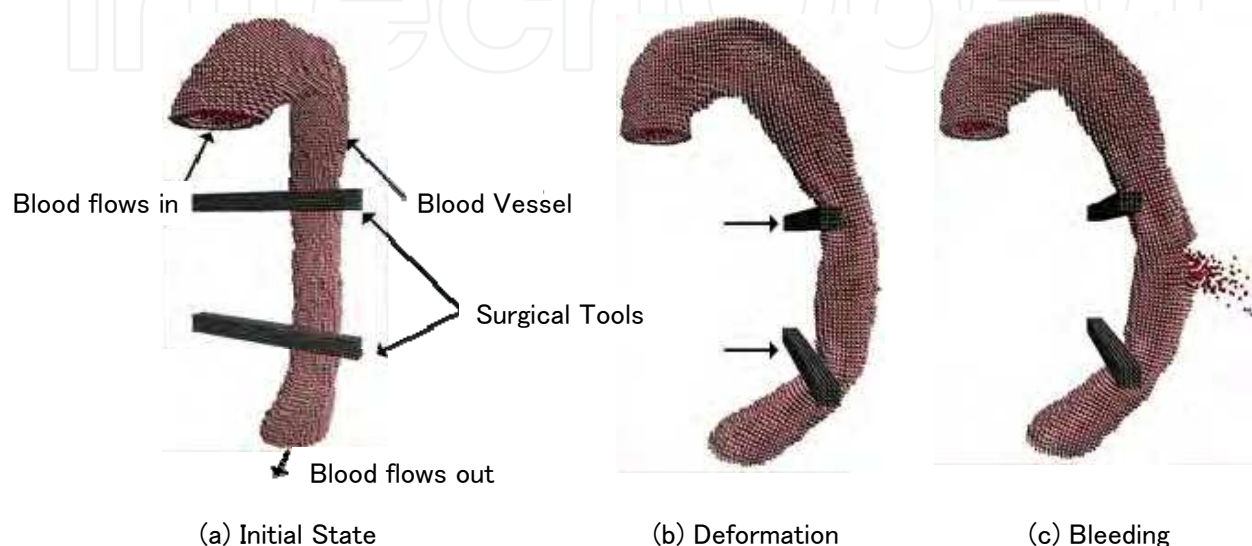
Fig. 11. Simulation of blood vessel deformation and bleeding

7. Conclusion

In this section, three kinds of simulation with particle method were explained. For all simulations, the basic equations are equation of continuity and Cauchy's equation of motion, which leads Navier-Stokes equation. There are two types of particle methods: SPH and MPS, and in this chapter these simulations use MPS method since MPS treats incompressible fluid such as water, viscoelastic fluid and blood. In bubble simulation, surface tension is added to Navier-Stokes equation so that the bubble moves up to water surface keeping its shape, and it is broken by the pressure from the inside of the bubble. In spinnability simulation, stress deviation of Cauchy's equation of motion is divided into two kinds: viscoelastic fluid and solvent. For stress deviation of viscoelastic fluid, two types of models, which are Giesekus and Larson models, were used to compare its stretching length. As the result of the simulation, stretching length with Larson model was longer than that of Giesekus's. Finally, blood vessel deformation and bleeding simulations were performed. Blood itself is fluid; however, blood vessel is elastic body so that the different equations of stress tensor were used for fluid and elastic body. Simulation result says that the blood vessel filled with blood flow is deformed moderately and bleeding simulation can be also visualized.

In the future, there are some issues to be solved. 1) three dimensional simulation of bubble moving, changing its shape, and disappearance, 2) considering a new model of stress deviation for viscoelastic fluid, which model stretches viscoelastic fluid longer and

expresses good spinnability, and 3) verification of the simulation of blood vessel deformation and bleeding. The simulation result should be evaluated by surgeons. In addition, visualization of the blood flow and stress distribution inside the blood vessel will be also useful for the preoperative planning of real surgeries.

8. Acknowledgment

9. References

Arimatsu K.; Nakagawa M & Mukai N. (2010). Particle Based Expression of Spinability of Viscoelastic Fluid, *Proceedings of the Media Computing Conference,* DVD, 4 pages

Chang Y.; Bao K.; Liu Y.; Zhu J. & Wu E. (2009). A Particle-based Method for Viscoelastic Fluids Animation, *Proceeding of the 16th ACM Symposium on Virtual Reality Software and Technology,* pp.111-117

Clavet S.; Beaudoin P. & Poulin P. (2005). Particle-based Viscoelastic Fluid Simulation, *Proceeding of the 2004 ACM SIGGRAPH/Eurographics Symposium on Computer Animation,* pp.219-228

Goktekin T. G.; Bargteil A. W. & O'Brien J. F. (2004). A Method for Animating Viscoelastic Fluids, *Proceeding of the 2004 ACM SIGGRAPH,* pp.463-468

Greenwood, S.T. & House D.H. (2004). Better with Bubbles : Enhancing the Visual Realism of Simulated Fluid, *Proceeding of the 2004 ACM SIGGRAPH/Eurographics Symposium on Computer Animation,* pp.287-296

Hong J. M.; Lee H. Y.; Yoon J. C. & Kim C. H. (2008). Bubbles Alive, *Proceeding of the 2008 ACM SIGGRAPH,* pp.48:1-48:4

Kagatsume N.; Nakagawa M. & Mukai N. (2011). Bubble Disappearance Simulation Using Particle Methods, *ITE Technical Report,* Vol. 35, No.32, pp.13-16

Kim B.; Liu Y.; Llamas I.; Jiao X. & Rossignac J. (2007). Simulation of Bubbles in Foam With The Volume Control Method, *Proceeding of the 2007 ACM SIGGRAPH,* pp.98-1-98-10

Kim D.; Song O. & Ko H. (2010). A Practical Simulation of Dispersed Bubble Flow, *Proceeding of the 2010 ACM SIGGRAPH,* pp.70:1-70:5

Koshizuka S. (2005), Particle Method, Maruzen Co. Ltd.

Losasso F.; Shinar T.; Selle A. & Fedkiw R. (2007). Multiple Interacting Liquids, *Proceeding of the 2006 ACM SIGGRAPH,* pp.812-819

Mukai N.; Ito K.; Nakagawa M. & Kosugi M. (2010). Sinnability Simulation of Viscoelastic Fluid, *the 2010 ACM SIGGRAPH posters*

Nakamura K. (1997), Non-Newtonian Fluid Mechanics, Corona Publishing Co. Ltd.

Nakagawa M.; Mukai N. & Kosugi M. (2010), A Blood Vessel Deformation Metho Considering Blood Stream for Surgical Simulations, *Proceeding of 2010 IWAIT,* CDROM, 6 pages

Nakagawa M.; Mukai N.; Tatefuku Y.; Niki K. & Takanashi S. (2011), Simulation of the Aorta Deformation and Bleeding by Using Particle Method, *Trans. of IIEEJ,* Vol. 40, No.5, pp.761-767

Qin J.; Pang W. M.; Nguyen B. P.; Ni D. & Chui C. K. (2010). Particle-based Simulation of Blood Flow and Vessel Wall Interaction in Virtual Surgery, *Proceeding of the 2010 Symposium on Information and Communication Technology,* pp.128-133

Selle A.; Rasmussen N. & Fedkiw E. (2005). A Vortex Particle Method for Smoke, Water and
          Explosions, *Proceeding of the 2005 ACM SIGGRAPH*, pp.910-914
Yamamoto K. (2009). Real Time Two-Way Coupling of Fluids to Deformable Bodies using
          Particle Method on GPU, *the 2009 ACM SIGGRAPH ASIA posters*
Zheng W.; Yong J. H. & Paul J. C. (2006). Simulation of Bubbles, *Proceeding of the 2006 ACM
          SIGGRAPH/Eurographics Symposium on Computer Animation*, pp.325-333
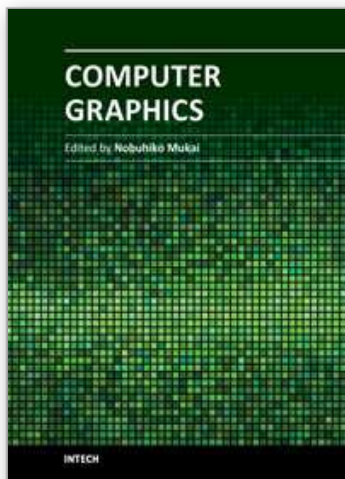
Computer Graphics

Edited by Prof. Nobuhiko Mukai

Computer graphics is now used in various fields; for industrial, educational, medical and entertainment purposes. The aim of computer graphics is to visualize real objects and imaginary or other abstract items. In order to visualize various things, many technologies are necessary and they are mainly divided into two types in computer graphics: modeling and rendering technologies. This book covers the most advanced technologies for both types. It also includes some visualization techniques and applications for motion blur, virtual agents and historical textiles. This book provides useful insights for researchers in computer graphics.

How to reference

In order to correctly reference this scholarly work, feel free to copy and paste the following:

Nobuhiko Mukai (2012). Simulations with Particle Method, Computer Graphics, Prof. Nobuhiko Mukai (Ed.), ISBN: 978-953-51-0455-1, InTech, Available from: http://www.intechopen.com/books/computer-graphics/simulations-with-particle-method

INTECH
open science | open minds